Ain Shams Engineering Journal (2014) 5, 657–666

Ain Shams University

Ain Shams Engineering Journal

www.elsevier.com/locate/asej
www.sciencedirect.com

CIVIL ENGINEERING

Numerical analysis of slid gate and neyrpic module intakes outflows in unsteady flow conditions

Rasool Ghobadian [a,*], Sabah Mohamadi [b], Sahere Golzari [c]

[a] *Water Engineering Department, Razi University of Kermanshah, Iran*
[b] *Hydraulic Structures Engineering, Razi University of Kermanshah, Iran*
[c] *Irrigation and Drainage Engineering, Razi University of Kermanshah, Iran*

Received 28 April 2013; revised 29 December 2013; accepted 11 February 2014
Available online 8 April 2014

KEYWORDS

Saint-Venant's equation;
Irrigation network;
Unsteady flow

Abstract Since the intakes outflow variations have an impact on network performance, it is necessary to evaluate the behavior of different types of intake structures in unsteady flow condition. In the present study, a computer model has been developed in which unsteady Saint–Venant flow equations have been discretized using finite difference and Crank–Nicolson method. Water surface elevation at junctions is calculated implicitly using matrix properties and influence line technique. After model verification, main channel of Miandarband irrigation network and its five branches were simulated. The result showed that without any operation instruction, a 10% decrease in the upstream flow discharge will reduce the slid gate, Neyrpic single orifice Module and double orifice Module intakes outflows for about 17.6%, 3.04% and 2.56%, respectively. With operation instruction, the maximum loss of flow volume is 707 m^3 during the first 10 h of operation for intake with slid gate.

1. Introduction

Opening and closing gates and water level regulating structures in irrigation networks establish unsteady flow in channels that adversely impacts the efficiency of these structures. The temporal and local variations in discharge along with the flow depth change produce a complex hydraulic condition in irrigation networks. Without using numerical models, accurate evaluation of flow pattern and behavior is very difficult. The water delivery irrigation channels must provide a sustainable and appropriate amount of flow to specific locations at suitable times. For any channel, this process is affected by the methods used to operate and control the channel and by rate of change in discharge. In order to shorten response time, limit water level fluctuation, and maintain the stability and performance of automatic control channel systems, appropriate automatic channel control methods should be adopted (Reddy, Blesa et al. and Fleiu et al.) [1–3]. The monitoring and control of water delivery is becoming an important subject recently. Studies have shown that channel automation may enhance the flexibility of a water delivery system, which will allow communities and agricultural planers to conserve water (Lozano et al.) [4].

* Corresponding author. Tel.: +98 9188332489.
E-mail addresses: Rsghobadian@gmail.com (R. Ghobadian), Sabah. Mohamadi@gmail.com (S. Mohamadi), sahere.golzari@gmail.com (S. Golzari).

Peer review under responsibility of Ain Shams University.

ELSEVIER Production and hosting by Elsevier

2090-4479 © 2014 Production and hosting by Elsevier B.V. on behalf of Ain Shams University.
http://dx.doi.org/10.1016/j.asej.2014.02.002

The main purpose of an automatic channel control is to optimize the water supply in order to match the expected demands at the offtake level. In practice and with the traditional management tools, it is very difficult to manage open-channel water conveyance and delivery systems, especially if there is a demand-oriented operation (Clemmens) [5]. Shang Yizi et al. [6] showed that the developed control system rather than the system in current used had considerable potential to closely match discharge at the downstream check structures with those orders by water users while maintaining the water level throughout the length of the channel. Channel automation has been developed for many years, to the point where most new channel designs and channel modernization plans have some level of automation (Rodriguez et al. and Ghumman et al.) [7,8]. Channel control algorithms have a fathomless effect on the overall efficiency of the channel projects. The water management can be improved by refining the channel control algorithms. Many channel control algorithms have been developed based on simulation (Lozano et al. and Clemmens and Strand) [4,9]. However, few algorithms have been implemented in the field (Aguilar et al.) [10]. Fengxiaobo and Wang Kang [11] presented a relationship between the automatic control method and stability of the open channel using a numerical simulation in unsteady flow conditions.

Channel automation has become a significant study area. However, many of studies only use numerical simulators, without having the possibility to test and verify their mathematical approaches with physical models. In this research efforts have been made to bridge the theory with the real word. Due to importance of unsteady flow conditions and its effects on irrigation networks, a computer model was prepared in which partial differential equations for non-uniform unsteady flow (Saint–Venant equation) are solved by finite difference method and alternative technique. Matrix properties and influence line technique have been employed to determine water surface elevation at any time step. The model is able to calculate and evaluate the effect of system inflow changes on intake or check structures discharges. The present model is capable of simulating flow in irrigation networks in the presence of hydraulic structures. This model would eliminate the requirements for the expensive filed studies. This model is also able to evaluate the operational routines and proposed modifications to optimize irrigation network management.

2. Material and methods

Ordinarily, Saint–Venant equations are used to define one-dimensional unsteady non-uniform flow in open channels. The Saint–Venant equations, momentum and continuity equations can be expressed as follows:

$$\frac{\partial Q}{\partial t} - \frac{2\beta Q T_W}{A}\frac{\partial Z}{\partial t} + \frac{2\beta Q q_L}{A} - \beta\frac{Q^2}{A^2}\frac{\partial A}{\partial x} = -gA\frac{\partial A}{\partial x} - g\frac{n_m^2 Q|Q|}{AR^{(4/3)}} \quad (1)$$

$$\frac{\partial Q}{\partial x} + T_W\frac{\partial Z}{\partial t} = q_L \quad (2)$$

where Q = discharge, A = flow area, Z = water surface elevation, T_w = water surface width, β = momentum coefficient, n_m = Manning's roughness, R = hydraulic radius, qL = lateral discharge per unit length of channel (input +, output −). Eqs. (1) and (2) are discretized using finite difference method. The length of network channels separately is divided to several nodes and is discretized in the form of staggered grid. Linear form of continuity equation on any node in the channel network is as follows (Eq. (3)):

$$a_{pi} \times Q_{i-1}^{n+1} + b_{pi} \times Z_i^{n+1} + c_{pi} \times Q_{i+1}^{n+1} = d_{pi} \quad (3)$$

where

$$a_{pi} = -\frac{\theta}{x_{i+1} - x_{i-1}} = -c_{pi} \; b_{pi} = \frac{T_{w_i}^n}{\Delta t}$$

$$d_{pi} = -\frac{(1-\theta)(Q_{i+1}^n - Q_{i-1)}^n}{x_{i+1} - x_{i-1}} + \frac{T_{W_I}^n \times Z_i^n}{\Delta t} + \frac{Q_{L_i}^{n+1}}{x_{i+1} - x_{i-1}}$$

Also momentum equation can be discretized for each grid as follows (Eq. (4)):

$$a_{mi} \times Z_{i-1}^{n+1} + b_{mi} \times Q_i^{n+1} + c_{mi} \times Z_{i+1}^{n+1} = d_{m_i} \quad (4)$$

where

$$a_{m_i} = -\frac{\beta Q_i^n T_{W_i}^n}{A_i^n \times \Delta t} - \frac{gA_i^n\theta}{x_{i+1} - x_{i-1}}$$

$$b_{mi} = \frac{1}{\Delta t} + \frac{2\beta\theta Q_{L_i}^{n+1}}{(x_{i+1} - x_{i-1})A_i^n} - \frac{\beta Q_i^n}{(A_i^n)^2} \times \frac{A_{i+1}^n - A_{i-1}^n}{x_{i+1} - x_{i-1}} + \frac{gQ_i^n n_{m_i}^2}{A_i^n R_i^{4/3}}$$

$$c_{mi} = -\frac{\beta Q^{n_i} T_W^{n_i}}{A_i^n \times \Delta t} + \frac{gA_i^n\theta}{x_{i+1} - x_{i-1}}$$

$$d_{mi} = \frac{Q_i}{\Delta t} + \frac{2\beta(1-\theta)Q_{L_i}^{n+1}}{(x_{i+1} - x_{i-1})A_i^n} - \frac{\beta Q_i^n T_W^{n_i}(Z_{i+1}^n + Z_{i-1}^n)}{A_i^n \Delta t} - gA_i^n(1-\theta)\frac{Z_{i+1}^n - Z_{i-1}^n}{x_{i+1} - x_{i-1}}$$

In Eqs. (3) and (4), n and $n+1$ indicate time step and θ is time related weight parameter. The discretization scheme is completely explicit as θ is set to zero or implicit as θ is set to one. Eq. (5) shows matrix form of all linearized momentum and continuity equation for a channel with discharge hydrograph and stage-discharge boundary condition for upstream and downstream, respectively.As shown in Eq. (5), right-side matrix is divided into three matrixes.

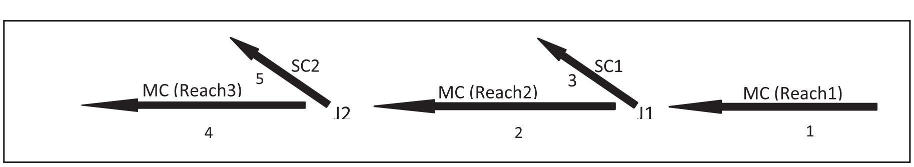

Figure 1 Channel branch of second order from main channel.

$$\begin{vmatrix} b_{p_2} & c_{p2} & 0 & 0 & 0 & 0 & 0 & 0 & 0 & 0 \\ a_{m3} & b_{m3} & c_{m3} & 0 & 0 & 0 & 0 & 0 & 0 & 0 \\ 0 & a_{p4} & b_{p4} & c_{p4} & 0 & 0 & 0 & 0 & 0 & 0 \\ 0 & 0 & a_{m5} & b_{m5} & c_{m5} & 0 & 0 & 0 & 0 & 0 \\ . & . & . & . & . & . & . & . & . & . \\ . & . & . & . & . & . & . & . & . & . \\ . & . & . & . & . & . & . & . & . & . \\ 0 & 0 & 0 & 0 & 0 & . & a_{m(n-3)} & b_{m(n-3)} & c_{m(n-3)} & 0 \\ 0 & 0 & 0 & 0 & 0 & 0 & 0 & a_{p(n-2)} & b_{p(n-2)} & c_{p(n-2)} \\ 0 & 0 & 0 & 0 & 0 & 0 & 0 & 0 & a_{m(n-1)} & b_{m(n-1)} \end{vmatrix} \begin{vmatrix} Z_2 \\ Q_3 \\ Z_4 \\ Q_5 \\ . \\ . \\ . \\ Q_{N-3} \\ Z_{N-2} \\ Q_{N-1} \end{vmatrix}^{t+\Delta t} = \begin{vmatrix} d_{p2} \\ d_{m3} \\ d_{p4} \\ d_{m5} \\ . \\ . \\ . \\ d_{m(n-3)} \\ d_{p(n-2)} \\ d_{m(n-1)} \end{vmatrix} + Q_1^{t+\Delta t} \times \begin{vmatrix} -a_{p2} \\ 0 \\ 0 \\ 0 \\ . \\ . \\ . \\ 0 \\ 0 \\ 0 \end{vmatrix} + Z_n^{t+\Delta t} \times \begin{vmatrix} 0 \\ 0 \\ 0 \\ 0 \\ . \\ . \\ . \\ 0 \\ 0 \\ -c_{m(n-1)} \end{vmatrix} \quad (5)$$

Considering only the first matrix, answers are given regardless upstream and downstream boundary conditions and are indicated by symbols $Q00$ or $Z00$. Second matrix with coefficient Q_1^{t+dt} (upstream input discharge at time $t + dt$) and third matrix with coefficient $(Z_n)^{t+dt}$ (downstream water surface elevation at time $t + dt$) show the effects of upstream and downstream boundary condition, respectively. For these conditions, answers are indicated in order by symbols $Q10/Z10$ and $Q01/Z01$. This method for separation right-side matrix into three matrixes, at first was used by Sobey et al. [12], well known as influence line technique. Also Ghobadian and Fathi-Moghadam used the influence line technique to develop a model for flood routing in complex ephemeral river systems [13].

2.1. Initial conditions

Initial flow depth and discharge in all of channels can be introduced to the model as initial conditions. In addition, in order to prevent of model divergence initial discharge of each secondary channel is calculated using stage-discharge relationship at the last cross-section with regard to initial water depth. Then main channel initial discharge at junction location is calculated using continuity equation. Input discharge to system in time step $n + 1$ is obtained with interpolating input hydrograph in any time step.

2.2. Open boundary condition

The most common boundary condition includes input hydrograph at upstream and stage-discharge relationship at downstream cross-section, which is obtained through uniform flow equations although other boundary conditions are also considerable. Input discharge at any $n + 1$ time steps is obtained from input hydrograph by interpolating and by using following equation obtained through discretizating continuity equation on the last cross section, water surface elevation for $n + 1$ time step on the last cross section enter equations system as downstream boundary condition.

$$Z_{ns}^{n+1} = Z_{ns}^{n} - \frac{\Delta t}{Tw_{ns}^{n}} \times \frac{Q_{ns}^{n} - Q_{ns-1}^{n}}{x_{ns} - x_{ns-1}} \quad (6)$$

In Eq. (6), index ns indicates the last cross section. Also, $(Z_n)^{ns}$ and $(Q_n)^{ns}$ are correlated through stage-discharge relation.

2.3. Internal boundary condition

In irrigation networks, location of intakes and water regulating structures are considered as internal boundary condition (e.g., J1 and J2 in Fig. 1). Different types of internal boundary condition are available depending on the intake location whether is upstream control or without control. for without control condition, according to continuity equation and equality of water surface at junction J1 [e.g., $Z(1,ns1) = Z(2,1) = Z(3,1) = Z_J$], governing equation at a junction is defined by Eq. (7), also for upstream control condition, by considering a relation between intake outflow discharge and junction water surface elevation governing equation at junction is written in Eq. (8):

$$\begin{aligned} F(J_1) &= Q_1 - (Q_2 + Q_3) \\ &= Q_{00}(1, ns_1 - 1) + Q_{10}(1, ns_1 - 1) \times Q(1,1) \\ &\quad + Q_{01}(1, ns_1 - 1) \times Z_{J2} - [Q_{00}(2,2) + Q_{10}(2,2) \\ &\quad \times Z_{J1} + Q_{01}(2,2) \times Z_{J2}] - [Q_{00}(3,1) + Q_{10}(3,1) \\ &\quad \times Z(3, ns_3)] \end{aligned} \quad (7)$$

$$\begin{aligned} F(J_1) &= Q_1 - (Q_2 + Q_3) \\ &= Q_{00}(1, ns_1 - 1) + Q_{10}(1, ns_1 - 1) \times Q(1,1) \\ &\quad + Q_{01}(1, ns_1 - 1) \times Z_{J2} - [Q_{00}(2,2) + Q_{10}(2,2) \\ &\quad \times Z_{J1} + Q_{01}(2,2) \times Z_{J2}] - [a_3 \times (Z_{J1} - Z_{03})^{b_3}] \end{aligned} \quad (8)$$

In Eqs. (7) and (8): $Q1$, $Q2$ and $Q3$ are discharge at the end of channel 1, beginning of channel 2 and beginning of channel 3, respectively. Q_{00} (1, ns1 – 1), Q_{10} (1, ns – 1) and Q_{01} (1, ns – 1) are discharge at (ns1 – 1)th cross section of channel 1, are obtained from solving matrix form for first, second and third matrixes at right side of Eq. (5), respectively. $Q(1,1)$ is input discharge from first section of channel 1 at time $t + dt$. Z_{J1} and Z_{J2} are water surface elevation at junction 1 and 2, respectively. $Q_{00}(2,2)$, $Q_{10}(2,2)$ and $Q_{01}(2,2)$ are discharge at second cross section of channel 2, are obtained from solving matrix form for first, second and third matrixes, $Q_{00}(3,1)$, $Q_{10}(3,1)$ Q and $Q_{01}(3,1)$ are discharge at first cross section of channel 3, are obtained from solving matrix form for first, second and third matrixes at right side of Eq. (5), respectively, $Z(3, ns_3)$ is water surface elevation at end section of channel 3, a_3 and b_3 coefficients are defined according to intake type, gate opening and weir length, and ultimately Z_{03} is intake sill elevation that for water surface elevation less than it at junction location, the inflow into channel 3 is zero.

For Neyrpic module, discharge variation against the water depth over weir crest enter as EXCEL file, and outflow of Neyrpic gate in time step $n + 1$ is taken with interpolating after water surface is calculated. If a radial gate is used, in free flow condition, outflow discharge is calculated using common equation (e.g. $q = c_d\sqrt{2gy_u}$ in which c_d is discharge coefficient and y_u is upstream depth) and in submerged flow condition using combination of energy and momentum equations well-known as E–M method can be calculated. A computer model is prepared in Visual Basic language in order to solve equations set and to obtain discharge and flow depth along channel reach, in which resulting 3-diagonal equation set is solved with 3-diagonal matrix algorithm (TDMA). To simplify in enter cross section data and downstream and upstream boundary conditions information, the Visual Basic program is linked with Excel program, as all of required data such as sections geometry data, roughness coefficients, input hydrograph as upstream boundary conditions and stage-discharge relation as downstream boundary condition were entered to Excel program, then these data are called by Visual Basic program. In general, this model was prepared for irregular geometry sections that also simply can simulate natural drainage networks.

2.4. Study area

The study was conducted in the Miandarband irrigation and drainage networks, located in the Kermanshah province of Iran. Main channel (MC) is extended from Razavar diversion dam to PC channel branch location. In addition, intakes of secondary channel were considered as simple intake, single orifice Neyrpic module and double orifice Neyrpic module. This network has five secondary channels. The plan of study area is shown in Fig. 2. The general characteristics of channels in this study are shown in Table 1.

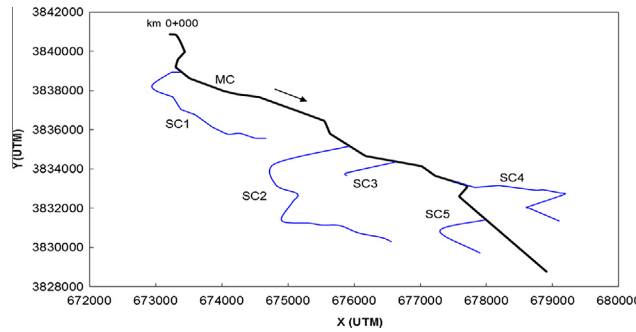

Figure 2 The plan of study area.

3. Discussion

3.1. Model verification

Very complex open channel system shown in Fig. 3 was used to study model ability for simulation gradually varied flow. Input discharge to system and flow depth at node 14 were 150 m^3/s and 5.0484 m, respectively. For all channel, Manning's coefficient was considered 0.013. Other characteristics of system are given in column 1–4 of Table 2. Value given in columns 5, 6 and 7 is discharge, flow depth at upstream node and flow depth at downstream node of each channel, respectively. By using calculated discharge and flow depths at the end of each channel (column 7) and calculations of gradually varied flow using standard step method (not provided here), flow depths at the upstream of each channel were calculated and compared with those provided in column 6 of the table.

Maximum error percentage was found to be 0.097% in channel 8. This indicates high accuracy of the model in simulating gradually varied flow within a complex network in which sometimes more than 7 branches enter or exit from one node. Even some famous models like HEC-RAS are not able to simulate it at all. The reason why depths calculated at node location are written with 6 decimal points is that, for comparing purpose, very small changes in flow depths at node location have considerable effects on channel discharge while calculating gradually varied flow.

Calculated discharge for channel 20 indicates that the direction of flow in Fig. 3 is incorrect, which was corrected by model calculations. Therefore the model is capable to correct the flow direction.

3.2. Simulation of unsteady flow

System shown in Fig. 3 is considered again. Hydrograph shown in Fig. 4a enters the system from node 1. Calculated discharge – stage relationship by model (using Manning's equation) was introduced to model as downstream boundary condition (at node 14). The model outputs are discharge hydrographs and stage hydrographs at different cross sections of each channel. Some of which are given in Fig. 4b as example.

As shown in Fig. 4, system input hydrograph has initial discharge and duration of 150 m^3/s and 40 h, respectively, the peak flow of which reaches 200 m^3/s within 17hr of occurring. Calculated peak flow of output hydrograph is 200 m^3/s and calculated time of peak flow appears 2880 s after the time of

Table 1 The general characteristics of channels.

Reach no.	Kilometer	Reach length (m)	Bed slope	Bed width (m)	Upstream structure	Downstream structure
1	0 – 2 + 510	2510	0.0014	4	Controlled input	Intake of Branch #1
2	2 + 510 – 7 + 235	4725	0.00028	4	–	Intake of Branch #2
3	7 + 235 – 8 + 282	1047	0.0003	4	–	Intake of Branch #3
4	8 + 282 – 9 + 642	1360	0.00078	4	–	Intake of Branch #4
5	9 + 642 – 11 + 741.91	2099.91	0.00029	4	–	Intake of Branch #5

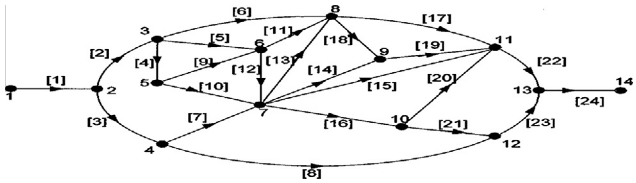

Figure 3 An example of river system.

peak of input hydrograph appears. The volume below output hydrograph is 23219997 m^3 having only a 0.000013% difference with input hydrograph volume (23220000 m^3), indicating very high accuracy of the model to satisfy continuity equation under unsteady flow conditions even in such a complex network. In this research, presented results of option five in (Monem and Massah) [14]are used to verify the model ability in unsteady flow simulation in irrigation single channel with types of intake and check structures. Monem et al. [15] by analyzing the unsteady flows in Dez irrigation network, operation instructions of E1R1 channel presented using ICSS hydrodynamic model. E1R1 channel with mean roughness coefficient equal to 0.017 has six intake structures and three check structures. Plan view of E1R1 channel and its related structures are shown in Fig. 5. The operational instructions of the hydraulic structures are given in Table 3. It can be seen that, input discharge to the channel (1 m^3/s) increases to 1.2 m^3/s because outflow discharge of intakes 5 and 6 change from 0.1 m^3/s to 0.2 m^3/s. At the first time (time = 0 h) the height of checks No. 2 and 3 are 0.1 m and 0.15 m respectively. Also the opening height of the gates No. 3, 4, 5 and 6 are 0.128 m. After one hr of the beginning of the operation the height of check No. 2 changes from 0.15 m to 0 and the gates No. 3 and 4 close a little so that their gate opening change to 0.217 m and 0.063 m respectively. After 2.2 h of the beginning of operation the opening of gates No. 5 and 6 increases from 0.128 m to 0.28 m.

Then flow behavior and discharge rate of intakes in 6-h schedule is determined.

Discharge changes over time in check structures location before and after apply operation conditions in option five are shown in Figs. 6 and 7. As shown in figures, the process of discharge changes over time in both model are similar and passed flow discharge on all three check structures is identical after establishment steady flow condition. Figs. 8 and 9 show changes in delivery discharge over time after apply operation changes for two intakes 5 and 6. There was a good accordance between present model results and ICSS model. Delivery final discharge rate in both of models was similar.

In unsteady time, present little differences between graphs can be caused by changes in discharge coefficient over changes in surface water elevation in intake location that in present study this coefficient is considered as constant.

3.3. Simulation of unsteady flow in Miandarband networks

After model verification, the sensitivity of difference intake structures to the deficit or surplus of water under unsteady condition in main channel of Miandarband network is examined. It is assumed that upstream input discharge decreases from 12 m^3/s to 10.8 m^3/s. Three types of intakes including simple slide gate, single orifice and double orifice NYERPIC module are used for water removal at the beginning of secondary channel. The water deficit rate in intakes on delivery 10 h program is computed. By assuming that intakes rate at any intakes of secondary channels changes according to row 6 in Table 4, without applying any operation option and with considering simple slide gate at beginning of secondary chan-

Table 2 Geometric characteristics of system shown in Fig. 3 and calculated values.

1 Channel number	2 Length (m)	3 Bed width (m)	4 Slope	5 Discharge (m^3/s)	6 Upstream depth (m)	7 Downstream depth (m)	8 Upstream depth GVF (m)
1	100	50	0.0005	150	4.603201	4.650808	4.601290
2	100	30	0.0004	74.7362	4.650808	4.690447	4.650868
3	257.5	40	0.0005	75.2638	4.650808	4.779108	4.651479
4	100	20	0.0004	26.28784	4.690447	4.730355	4.690531
5	150	25	0.00052	29.34708	4.690447	4.768352	4.690531
6	277.5	20	0.0005	19.10127	4.690447	4.829334	4.690684
7	65	30	0.0005	27.71652	4.779108	4.811583	4.779620
8	340	40	0.0005	47.54728	4.779108	4.944147	4.774434
9	100	50	0.00039	9.653419	4.730355	4.768352	4.729279
10	162.5	30	0.0005	16.63443	4.730355	4.811583	4.730347
11	150	40	0.0004	18.44252	4.768352	4.829334	4.769399
12	125	40	0.00034	20.55799	4.768352	4.811583	4.769094
13	70	20	0.00025	0.344822	4.811583	4.829334	4.811808
14	75	30	0.0005	10.09849	4.811583	4.849079	4.811656
15	175	30	0.0005	19.99483	4.811583	4.899049	4.811656
16	125	40	0.0005	34.47078	4.811583	4.874292	4.811808
17	140	30	0.0005	22.69812	4.829334	4.899049	4.829046
18	40	30	0.0005	15.19049	4.829334	4.849079	4.829046
19	100	30	0.0005	25.28898	4.849079	4.899049	4.849030
20	50	30	0.0005	−10.9964	4.874292	4.899049	4.874049
21	100	20	0.0007	45.46717	4.874292	4.944147	4.874201
22	200	30	0.0005	56.98554	4.899049	4.998756	4.899067
23	100	50	0.0005	93.01446	4.944147	4.998756	4.948951
24	100	50	0.0005	150	4.998756	5.0484	4.998682

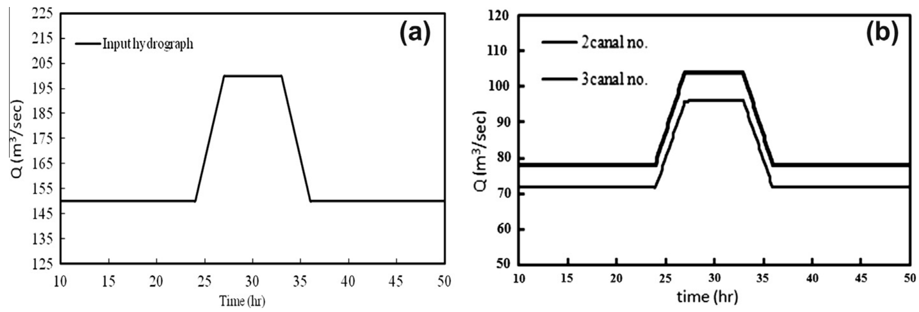

Figure 4 (a) System input/output hydrograph, (b) discharge hydrographs calculated at the beginning of channel 2 and 3.

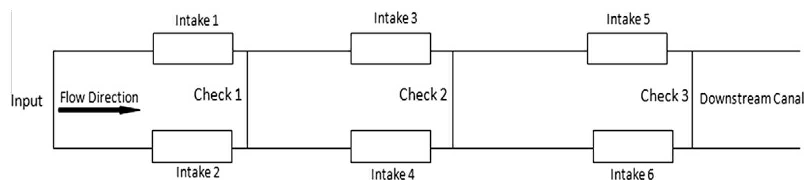

Figure 5 The schematic of E1R1 channel and existing structures in reach.

Table 3 The regulating instructions of structures.

Input discharge to main channel (m^3/s)	Exit discharge of main channel (m^3/s)	Discharge of intake #5 (m^3/s)	Discharge of intake #6 (m^3/s)	Discharge of intake #3 (m^3/s)	Discharge of intake #4(m^3/s)	
Initial condition						
1	0.6	0.1	0.1	0.1	0.1	
Operational instructions						
Time (h)	The height of check #3 (m)	Gate opening at intake #5 (m)	Gate opening at intake #6 (m)	The height of check #2 (m)	Gate opening at intake #3 (m)	Gate opening at intake #4 (m)
0	0.1	0.128	0.128	0.15	0.066	0.233
1	0.1	0.128	0.128	0	0.063	0.217
2.2	0.1	0.28	0.28	0	0.063	0.217
Final condition						
Input discharge to main channel (m^3/s)	Exit discharge of main channel (m^3/s)	Discharge of intake #5 (m^3/s)	Discharge of intake #6 (m^3/s)	Discharge of intake #3 (m^3/s)	Discharge of intake #4(m^3/s)	
1.2	0.6	0.2	0.2	0.1	0.1	

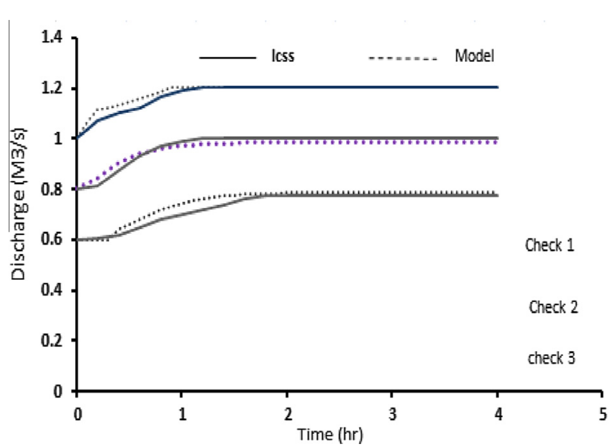

Figure 6 Changes in discharge over time in check structures before operating.

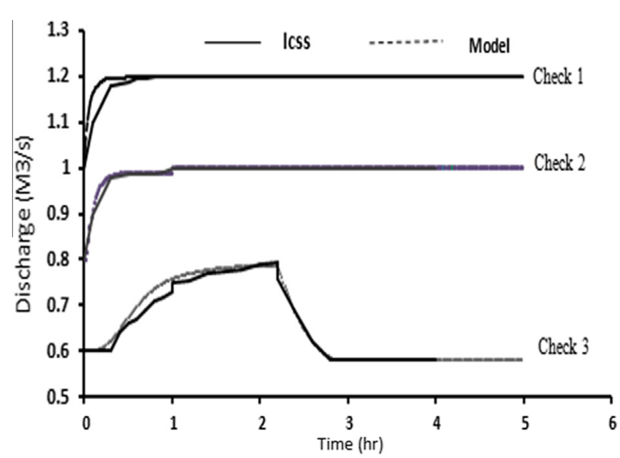

Figure 7 Changes in discharge over time in check structures after operating.

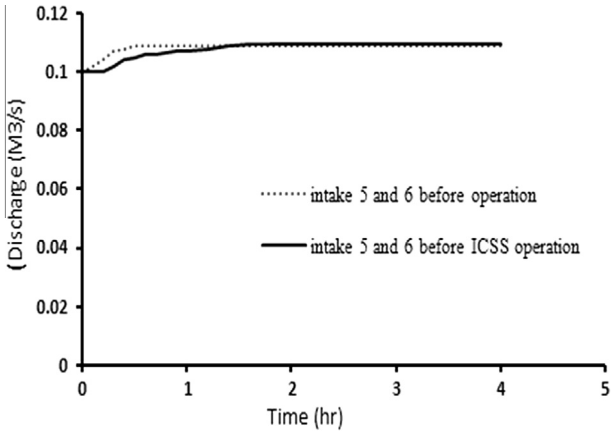

Figure 8 Changes in discharge over time in intake 5 and 6 before operating.

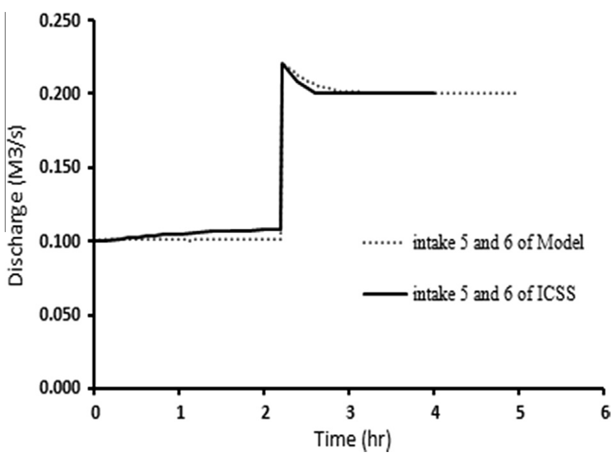

Figure 9 Changes in discharge over time in intake 5 and 6 after operating.

nels, parameter (a) values that showing gates opening value of secondary channels was calculated by trial and error method and run model repeatedly which can be presented in second row in Table 5. Note that presented parameters in Table 4 are the coefficients of intake discharge relation $z = aQ^b$. Parameter (b) depending on intake type, simple or NEYRPIC module has a value between 0.5 to 1.5 that in this study has selected as 0.5. In two other difference cases, single and double orifice NYERPIC modules placed at beginning of secondary channel in which discharge rate is similar with slide gates that mentioned above, and no slide gate is opened and closed after decreasing upstream discharge. Note that in this study SC1, SC3, SC5 secondary channels intakes from XX module type and SC3, SC4 channels from L module type have been selected. In Table 5, losses of passed discharge of intakes have been given in the three cases mentioned. The results indicated that by decrease in upstream discharge, simple intakes have shown the maximum sensitivity in comparison with single orifice and double NYERPIC module. This means that with decrease of 10% upstream discharge, water removal rate of simple intakes 6.17% and in single orifice NYERPIC module 3.04% decrease while, change rate of water removal of double NYERPIC module decreases 2.56%.

In another step, the purpose is finding the decrease of 10% the end discharge of main channel that convey to the downstream meanwhile discharge of branched tributary channels from main channel decrease 10% as well. Under this condition, input discharge and end discharge of main channel from 12 to 10.08 m^3/s and from 9.9 to 8.91 decreases respectively. Due to decreasing of input discharge to main channel and requirement decrease in tributary channels similarly, it is necessary that gate opening rate of tributary channels intake changes. The difference options of operation on network can be applied to decreasing of error rate of passed discharge. An operation option not necessarily optimal option is that the opening of intakes changes with input discharge rate of upstream simultaneously. For these conditions, the changes percent of gates opening at any tributary channels have been determined by comparison of parameter (a) values after, before operation apply and change in input discharge. As seen in Table 4, the most decrease in opening rate of intake at the beginning of SC2 channel is nearly 9.02%. The changes in discharge rate at NYERPIC gates after, before applying operation is according to row 6 and 7 in Table 4. We know that different types of NYERPIC gates are including several slide gates with different discharges. For decrease 10% of passed discharge of NYERPIC gates, existing gates are completely closed based on water requirement rate in desired time. As the upstream discharge decreases to 10.8 m^3/s, two slide gates 20 Lit in intake of SC1 channel, one slide gates 50Lit in intake of SC2 channel, one slide gates 20 Lit and one slid gate 10 Lit in intake of SC3 channel, one slide gates 50 Lit in intake of SC4 channel and two slide gates 50 Lit in intake of SC5 channel are closed completely. Figs. 10–15 show the values of delivery discharge in varied times after applying operation changes in any tributary channel intakes.

As it can be seen from Fig. 15 the value of discharge at downstream channel decreased from 9.9 to 8.91 m^3/s by 10%. Error in volume through at the beginning of branches

Table 4 Secondary channel characteristics before and after applying operation instruction.

Channel characteristics	Channel				
	Sc1	Sc2	Sc3	Sc4	Sc5
Parameter "a" before operation	0.519	0.706	0.447	0.588	0.479
Parameter "a" after operation	0.504	0.69	0.434	0.562	0.46
Parameter "b"	0.5	0.5	0.5	0.5	0.5
Increasing of intake opening (%)	2.89	9.02	2.9	4.42	3.96
Discharge of channel before operation (M^3/s)	0.4	0.5	0.3	0.5	0.4
Discharge of channel after operation (M^3/s)	0.36	0.45	0.27	0.45	0.36

Table 5 The losses of outflow discharge of intakes.

	Simple intake	Single orifice Neyrpic module	Double orifice Neyrpic module
Losses of outflow discharge (M^3/s)	4667.04	2298.24	1935.36
Percent decrease in outflow discharge (%)	6.17	3.04	2.56

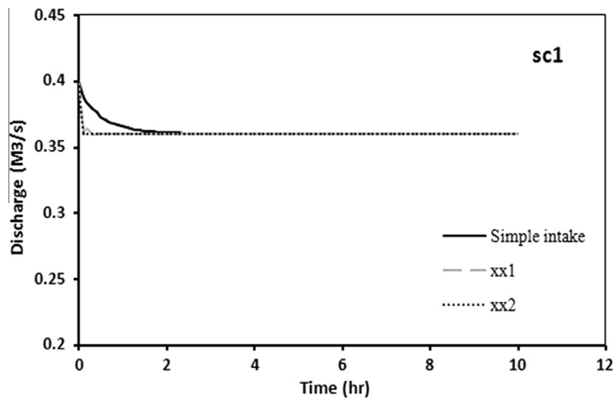

Figure 10 Changes in discharge over time at beginning intake of SC1 channel.

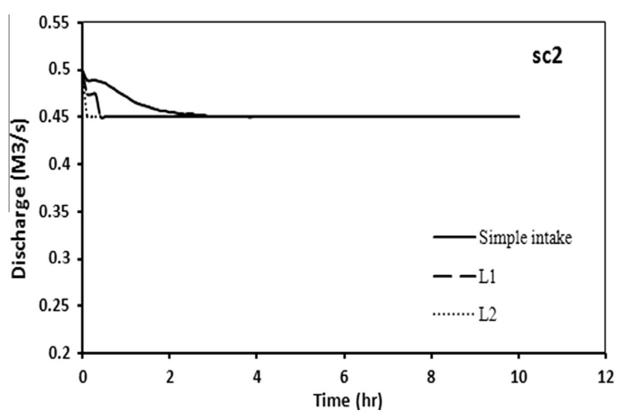

Figure 11 Changes in discharge over time at beginning intake of SC2 channel.

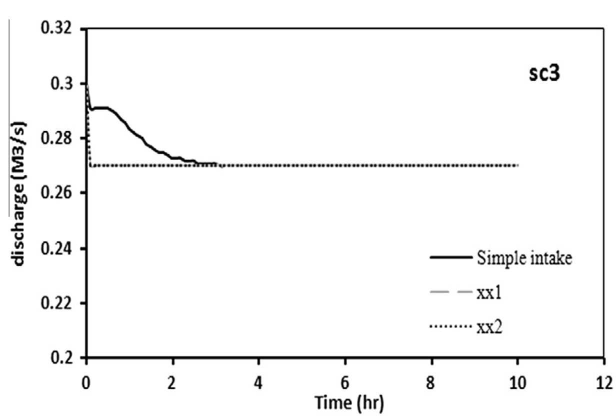

Figure 12 Changes in discharge over time at beginning intake of SC3 channel.

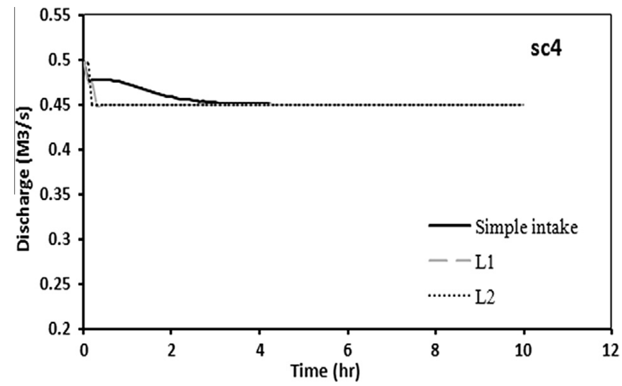

Figure 13 Changes in discharge over time at beginning intake of SC4 channel.

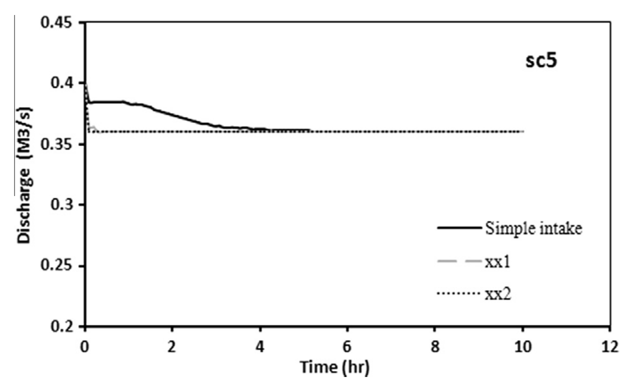

Figure 14 Changes in discharge over time at beginning intake of SC5 channel.

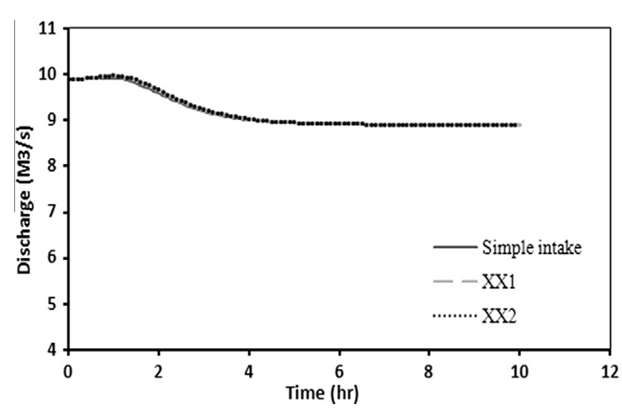

Figure 15 Changes in discharge over time at beginning intake of SC6 channel.

Table 6 Most losses of flow volume through in intakes.

	Simple intake	Single orifice Neyrpic module	Double orifice Neyrpic module
Error in passed volume (m^3)	707.04	45	32.2

in the three conditions which intake structure is replaced presented in Table 6.

As it can be observed the most losses of passed flow volume of simple intakes is 707.04 m^3 at first 10 h operation. Single orifice and double NYERPIC module in compare to simple intake decrease the percent losses of flow volume to 93.63 and 95.44 respectively. The flow losses volume double NYERPIC module is 28.44% less than single orifice NYERPIC module which indicating better performance of double NYERPIC module at Mc channel of Miandarband network.

4. Conclusions

In this paper a computer model has prepared that can be used to operating irrigation networks. This model is able to evaluate the effects of input discharge decrease or increase to the system on intakes discharge. Also this model enables to calculate the reach time and unsteady condition continuity in every intakes location. From this paper the following conclusions can be obtained:

(1) Without any operation instruction, a 10% decrease in the upstream flow discharge will reduce the discharge of intakes with slid gate and single orifice Neyrpic module 6.17% and 3.04% respectively. Also Flow passing of double orifice Neyrpic module gate will reduce 2.56%.
(2) With carrying out operation instruction during initial 10 h, the most losses of passed flow volume of simple intakes at secondary channel are 707 m^3. This value for single and double orifice Neyrpic module is 45 m^3 and 32.2 m^3 respectively.

References

[1] Reddy JM. Evaluation of optimal constant-volume control for irrigation channels. Appl Math Model 1990;14(9):450–8.
[2] Blesa J, Puig V, Bolea Y. Fault detection using interval LPV models in an open-flow channel. Control Eng Practice 2010;18(5):460–70.
[3] Fleiu-Battle V, Rivas Perez R, Sanchez Rodriguez L. Fractional robust control of main irrigation channels with variable dynamic parameters. Control Eng Practice 2007;15(6):673–86.
[4] Lozano D, Arranj C, Rijo M, et al. Simulation of automatic control of an irrigation channel. Agric Water Manage 2010;97(4):91–100.
[5] Clemmens AJ. Delivery system schedules and required capacities. In: Zimbelman DD, editors. Planning, operation, rehabilitation and automation of irrigation water delivery systems ASCE, New-York; 1987. p. 18–34.
[6] Shang Yizi, Rogers Peter, Wang Guang Qian. Design and evaluation of control systems for a real canal. Technol Sci 2012;55(7):142–54.
[7] Rodriguez CE, Patterson CG, Hesla E. Panama channel control system. IEEE Ind Appl Mag 2009;15(2):8–11.
[8] Ghumman AR, Khan MZ, Khan AH. Assessment of operational strategies for logical and optimal use of irrigation water in a downstream control system. Irrig Drain 2010;59(5):117–28.
[9] Clemmens AJ, Strand RJ. Downstream water level control test results on the WM lateral channel. J. Irrig Drain E – ASCE 2010;136:460–9.
[10] Aguilar JV, Langarita P, Linares L, et al. Automatic control of flows and levels in an irrigation channel. IEEE T Ind Appl 2009;45:2198–208.
[11] Feng Xiaobo, Wang Kang. Stability analysis on automatic control methods of open channel. J Natural Sci 2011;16:325–31.
[12] Sobey RJ, Adil TS, Vidler PF. User's Guide to ESTFLO/Version2B. James Cook University of North Queensland, Department of Civil and System, Engineering, Research, Bulletin No. CS22; 1980.
[13] Ghobadian R, Fathi-Moghadam M. Estimation of seepage losses in ephemeral network and branching streams. J Hydrologic Eng 2013. http://dx.doi.org/10.1061/ (ASCE) HE.1943-5584.0000788 (Jan. 19.
[14] Monem M, Massah A. Numerical model in Neyrpic Module. Eleventh Cong Iranian Natl Committee Irrigat Drain 2003;42.
[15] Monem M, Emadi A, Ghodosi H. Evaluating of unsteady flow in irrigation network and determining appropriate operation instructions. Agric-Eng Res J 2006; 24(6) [in Persian].

Rasool Ghobadian earned his BS degree in irrigation and engineering in 1997, from Shahid Chamran University, Ahvaz, Iran with first ranking. He has earned his M.S. degree and his Ph.D degree in Hydraulic Structures Engineering from Shaid Chamran university of Ahvaz and Tehran University in 2000 and 2007 respectively. He is currently employing in department of water engineering, Razi University, Kermanshah, Iran as assistant professor. His main research interests include numerical modeling of unsteady flow in irrigation network and river systems, design of Hydraulic Structure and river engineering. He has published more than a hundred papers in these areas of expertise.

Sabah Mohamadi earned his BS degree in irrigation and engineering in 2009, from Razi university of Kermanshah, Iran and his M.S. degree in Hydraulic Structures Engineering in 2011 from Shahid Chamran university of Ahvaz, Iran. He is currently a Ph.D degree student of hydraulic structures engineering at Razi University, Iran. His main research interests include Hydraulic Structures, irrigation networks and he has written several papers in these areas of expertise.

Sahere Golzari earned her BS degree in water engineering in 2009, from Uremia University, Uremia, Iran and her M.S. degree in irrigation and drainage engineering in 2010 from Razi university of Kermansha, Iran. She is currently a Ph.D degree student of irrigation and drainage engineering at Bu Ali Sina University, Hamadan, Iran. Her main research interests include numerical simulation of unsteady flow in irrigation networks and she has published several papers in these areas of expertise.